CONFIDENTIAL

Copy 180
RM L9D06

NACA RM L9D06

NACA

RESEARCH MEMORANDUM

WIND-TUNNEL INVESTIGATION AT HIGH SUBSONIC SPEEDS OF THE LATERAL-CONTROL CHARACTERISTICS OF AN AILERON AND A STEPPED SPOILER ON A WING WITH LEADING EDGE SWEPT BACK 51.3°

By

Leslie E. Schneiter and John R. Hagerman

Langley Aeronautical Laboratory
Langley Air Force Base, Va.

CLASSIFICATION CHANGED TO
UNCLASSIFIED DATE 8-18-54
AUTHORITY J.W.CROWLEY
CHANGE #2428 J.C.

CLASSIFIED DOCUMENT

This document contains classified information affecting the National Defense of the United States within the meaning of the Espionage Act, USC 50:31 and 32. Its transmission or the revelation of its contents in any manner to an unauthorized person is prohibited by law. Information so classified may be imparted only to persons in the military and naval services of the United States, appropriate civilian officers and employees of the Federal Government who have a legitimate interest therein, and to United States citizens of known loyalty and discretion who of necessity must be informed thereof.

NATIONAL ADVISORY COMMITTEE FOR AERONAUTICS

WASHINGTON

June 7, 1949

CONFIDENTIAL

NATIONAL ADVISORY COMMITTEE FOR AERONAUTICS

RESEARCH MEMORANDUM

WIND-TUNNEL INVESTIGATION AT HIGH SUBSONIC SPEEDS OF THE LATERAL-CONTROL CHARACTERISTICS OF AN AILERON AND A STEPPED SPOILER ON A WING WITH LEADING EDGE SWEPT BACK 51.3°

By Leslie E. Schneiter and John R. Hagerman

SUMMARY

A wind-tunnel investigation has been made through a speed range from a Mach number of 0.30 to a Mach number of approximately 0.90 to determine the lateral-control characteristics of a 20-percent-chord by 39-percent-semispan aileron and a 60-percent-semispan stepped spoiler on a semispan-wing model with aspect ratio of 3.06 having 51.3° sweepback of the wing leading edge. In addition, the aerodynamic characteristics of the plain wing were determined through the speed range.

The aileron rolling effectiveness decreased as the Mach number increased; whereas the spoiler rolling-moment effectiveness increased with Mach number. The increase of rolling-moment coefficient with spoiler projection was nearly linear at wing angles of attack of 0° and 4°.

The hinge-moment parameters C_{h_α} and $C_{h_{\delta_{a_T}}}$ (slope of the curves of hinge-moment coefficient with wing angle of attack and aileron deflection, respectively) were negative and varied almost negligibly with variation of the Mach number.

INTRODUCTION

The importance of obtaining adequate lateral control for airplanes incorporating sweptback wings has led the NACA to engage in an extensive program of lateral-control research on various sweptback-wing configurations. The purposes of this program are to determine the characteristics of various lateral-control devices, to attempt to improve these characteristics where possible by modification of these devices, and to investigate wholly new lateral-control devices.

Reported herein are the results of a lateral-control investigation of a 20-percent-chord by 39-percent-semispan sealed plain aileron on a 51.3° sweptback wing having an aspect ratio of 3.06 and a taper ratio of 0.49. The lateral-control characteristics of two stepped spoilers, similar to spoiler 18 of reference 1, were also investigated.

Aileron rolling-moment, yawing-moment, and hinge-moment coefficients were determined through a speed range from a Mach number of 0.30 to a Mach number of 0.91 over a range of aileron deflection of approximately ±30° and a range of wing angle of attack from approximately -4° to 16°. Spoiler rolling-moment and yawing-moment coefficients were determined for both spoiler configurations at one spoiler projection through the speed range and at wing angles of attack from approximately -4° to 4°. The characteristics of the more satisfactory of the two spoiler configurations were determined through a range of spoiler projections.

The tests were made in the Langley high-speed 7- by 10-foot tunnel.

DEFINITIONS AND SYMBOLS

The forces and moments on the wing are presented about the wind axes, which for the conditions of these tests (zero yaw) correspond to the stability axes. (See fig. 1.) The axes intersect at a point 26.6 inches rearward of the leading edge of the wing root on the line of intersection of the plane of symmetry and the chord plane of the model, as shown in figure 2. This corresponds to a point 26.2-percent chord rearward of the leading edge of the wing mean aerodynamic chord, as also shown in figure 2.

The rolling-moment and yawing-moment coefficients determined on the semispan wing represent the aerodynamic effects that occur on a complete wing as a result of deflection of the aileron or projection of the spoiler on only one semispan of the complete wing. The lift, drag, and pitching-moment coefficients determined on the semispan wing (with the aileron or spoiler neutral) represent those that occur on a complete wing.

The symbols used in the presentation of results are as follows:

C_L lift coefficient $\left(\frac{\text{Twice lift of semispan model}}{qS}\right)$

C_D drag coefficient $\left(\frac{\text{Twice drag of semispan model}}{qS}\right)$

C_m pitching-moment coefficient $\left(\frac{\text{Twice pitching moment of semispan model}}{qS\bar{c}}\right)$

C_l rolling-moment coefficient $\left(\frac{L}{qSb}\right)$

C_n yawing-moment coefficient $\left(\frac{N}{qSb}\right)$

C_h aileron hinge-moment coefficient $\left(\frac{H_a}{2q \times \text{Area moment of aileron rearward of and about aileron hinge axis}}\right)$

c local wing chord measured in planes parallel to wing plane of symmetry

c' local wing chord measured in planes perpendicular to wing 0.556c line

$\bar{c}$ wing mean aerodynamic chord, 2.087 feet $\left(\frac{2}{S}\int_0^{b/2} c^2 dy\right)$

c_a local aileron chord measured along wing-chord plane from hinge axis to trailing edge of aileron in planes parallel to wing plane of symmetry

c_a' local aileron chord measured along wing-chord plane from hinge axis of aileron to trailing edge of aileron in planes perpendicular to wing 0.556c line

b twice span of semispan model, 6.066 feet

y lateral distance from plane of symmetry, feet

S twice area of semispan model, 12.06 square feet

L rolling moment due to aileron deflection, foot-pounds

N yawing moment due to aileron deflection, foot-pounds

H_a aileron hinge moment, foot-pounds

q free-stream dynamic pressure, pounds per square foot $\left(\frac{1}{2}\rho V^2\right)$

V free-stream velocity, feet per second

ρ mass density of air, slugs per cubic foot

α angle of attack with respect to chord plane at root of model, degrees

δ_{a_T} true aileron deflection corrected for deflection under load, relative to wing-chord plane and measured in planes perpendicular to aileron hinge axis, degrees

$\delta_{a_{ave}}$ average true deflection of aileron $\left(\delta_{a_T}\right)$ throughout Mach number range

M Mach number

R_N Reynolds number

$C_{h_\alpha} = \left(\frac{\partial C_h}{\partial \alpha}\right)_{\delta_{a_T}}$

$C_{h_{\delta_{a_T}}} = \left(\frac{\partial C_h}{\partial \delta_{a_T}}\right)_\alpha$

$C_{L_\alpha} = \left(\frac{\partial C_L}{\partial \alpha}\right)_{\delta_{a_T}}$

$C_{l_{\delta_{a_T}}} = \left(\frac{\partial C_l}{\partial \delta_{a_T}}\right)_\alpha$

The subscripts δ_{a_T} and α indicate the factor held constant. All slopes were measured in the vicinity of 0° angle of attack and 0° aileron deflection.

CORRECTIONS

The test data have been corrected for jet-boundary and reflection-plane effects by the method of reference 2. Compressibility effects on these jet-boundary and reflection-plane corrections have been considered in correcting the test data. Blockage corrections as determined from reference 3 to account for the constriction effects of the model on the tunnel free-stream flow were also applied.

Aileron deflections have been corrected for deflection under load, and the aileron and spoiler rolling-moment-coefficient data have been corrected for the wing twist produced by aileron deflection or spoiler projection.

APPARATUS AND MODEL

The tests were made in the Langley high-speed 7- by 10-foot tunnel which is a closed-throat, single-return tunnel capable of reaching choking Mach number.

The cantilever semispan sweptback-wing model was mounted in the tunnel, as shown in figure 3. The root chord of the model was adjacent to the ceiling of the tunnel, the ceiling thereby serving as a reflection plane. The model was mounted on the balance system in such a manner that all forces and moments acting on the model could be measured. A small clearance was maintained between the model and the tunnel ceiling so that no part of the model came in contact with the tunnel structure. A small

end plate was attached to the root of the model to deflect the spanwise flow of air that enters the tunnel test section through the clearance hole between the model and the tunnel ceiling.

The model used for these tests was built of aluminum to the planform dimensions shown in figure 2. The model had an aspect ratio of 3.06, a taper ratio of 0.49, and the leading edge of the model was swept back 51.3°. The wing sections perpendicular to the 55.6-percent-chord line were of NACA 65-012 airfoil profile.

The model was equipped with a 20-percent-chord by 39-percent-semispan true-contour sealed plain aileron, the outboard end of which was located 6.8 percent of the wing semispan inboard from the wing tip. The aileron had a semicircular nose and was internally sealed with plastic-impregnated cloth attached to both the wing and the aileron nose across the gap ahead of the control-surface nose except at the hinge stations. Although no seal-leakage measurements were made, it is believed that the seal was fairly complete. The aileron hinge moments were measured with an electric resistance-type strain gage.

The two spoiler configurations investigated were each composed of six equal-span spoiler segments placed perpendicular to the free-stream air flow with the center of each segment on the wing 0.70c line. To form the two configurations investigated, the six spoiler segments were placed from the $0.20\frac{b}{2}$ to the $0.80\frac{b}{2}$ wing stations and from the $0.30\frac{b}{2}$ to the $0.90\frac{b}{2}$ wing stations; these two spoiler arrangements are hereinafter referred to as spoiler configuration 1 and configuration 2, respectively. A sketch of spoiler configuration 1 is shown in figure 4.

TESTS

The Mach number range for the tests was from about $M = 0.30$ to about $M = 0.91$, which corresponds to a Reynolds number range from $R_N = 4.22 \times 10^6$ to $R_N = 9.34 \times 10^6$ based on a mean aerodynamic chord length of 2.087 feet. The variation of Reynolds number with Mach number is shown in figure 5.

Wing angle-of-attack tests with the aileron at $\delta_{a_T} = 0^\circ$ were made at various constant Mach numbers through an angle-of-attack range from approximately -4° to wing stall at $M = 0.30$ and to approximately 8° at all other Mach numbers.

Aileron lateral-control tests were made at constant angles of attack from -4° to 16° through the Mach number range with the aileron at constant deflections ranging from approximately $\delta_{a_{ave}} = -30$ to 30°. The spoiler lateral-control tests were made at constant angles of attack from approximately -4° to 4° through the Mach number range with the spoiler at

constant projections. Spoiler configuration 1 was investigated at projections of $-\frac{1}{2}$, -1, -2, -3, -5, and -7 percent chord; whereas spoiler configuration 2 was investigated only at a projection of -7 percent chord. (Spoiler projection is negative when spoiler projects above wing upper surface.)

RESULTS AND DISCUSSION

The results of the investigation are presented in figures 6 to 11.

Wing Aerodynamic Characteristics

Lift characteristics.- The curves of lift coefficient against wing angle of attack for all Mach numbers (shown in fig. 6) were linear through the low angle-of-attack range. At a Mach number of 0.30 (the only Mach number at which data were obtained at high angles of attack) and $\alpha \approx 8^{\circ}$ ($C_L \approx 0.44$) the slope C_{L_α} increased slightly with increasing angle of attack to an angle of attack of about 12.5° ($C_L \approx 0.66$) past which point the slope C_{L_α} decreased continuously to maximum lift which occurred at an angle of attack of about 25° where a lift coefficient of $C_L \approx 0.99$ was obtained. The conditions for a lift-force break were not reached within the limited angle-of-attack range investigated at the higher Mach numbers.

The slope C_{L_α} increased with increasing Mach number from a value of 0.048 at $M = 0.30$ to a value of 0.057 at $M = 0.90$ as shown in figure 7. The experimentally determined variation of C_{L_α} with Mach number is compared in figure 7 with the theoretical slope C_{L_α} as predicted by the method of reference 4. The agreement between the experimental and theoretical values of C_{L_α} is considered excellent inasmuch as the discrepancies between the values at any Mach number are within the experimental accuracy of determining C_{L_α}. The data of figure 6 show that the angle of attack for zero lift is slightly negative and not zero as would be expected for a wing having a symmetrical airfoil. This phenomenon is merely the result of slight misalinement of the model and air stream and in no way affects the slope C_{L_α}.

Drag characteristic.- The drag coefficient for any constant lift coefficient (fig. 6) increased with increasing Mach number to the highest speed investigated ($M \approx 0.91$) but indicated that the critical speed of the wing near zero lift was not reached.

Pitching-moment characteristics.- For the angle-of-attack range wherein lift varied linearly with angle of attack, the pitching-moment coefficient varied almost linearly with angle of attack (or lift

coefficient) as shown in figure 6. For the angle-of-attack range wherein C_{L_α} increased slightly, the stability of the wing, as indicated by the slope of the curve of pitching-moment coefficient against lift coefficient $\partial C_m/\partial C_L$, also increased. At a lift coefficient of about 0.66, the lift-curve slope, as noted previously, started to decrease and the wing became unstable. In the low lift-coefficient range, the stability of the wing increased slightly with increasing Mach number.

Aileron Lateral-Control Characteristics

Rolling moment.- The aileron rolling effectiveness generally increased with increasing aileron deflection and decreased with increasing wing angle of attack and/or Mach number. (See figs. 8 and 9.) The decreasing effectiveness of the aileron with increasing Mach number is at variance with theory (such as the Prandtl-Glauert relations), which would predict increasing aileron effectiveness with increasing Mach number, but is in agreement with the results obtained for ailerons on some swept wings. The discrepancy between theory and experimental data apparently results from the inability of the theory to predict the spanwise shift in center of pressure of the flap load with increasing Mach number.

Since the foot-pounds of aileron hinge moment increased with increasing Mach number and the aileron restraining mechanism was somewhat flexible, the true deflection of the aileron δ_{a_T} decreased with increasing Mach number. The individual test-point values of the moment coefficients presented in figure 8 are the values for the true aileron deflection δ_{a_T}, which may vary by as much as 1° from the average deflection $\delta_{a_{ave}}$ noted on the figure. As a consequence, cross plotting of the data of figure 8 against $\delta_{a_{ave}}$ to determine the control parameters $C_{h_{\delta_{a_T}}}$ and $C_{l_{\delta_{a_T}}}$ will result in values of these parameters slightly higher at low Mach numbers and lower at high Mach numbers than the values presented on figure 9 which were determined using the actual control-surface deflections.

The aileron-effectiveness parameter $C_{l_{\delta_{a_T}}}$ was estimated for this aileron by Method I of reference 5, and a comparison of the calculated and the experimental values at the minimum Mach number investigated (0.30) is shown in figure 9. The results agree within the accuracy with which the experimental values may be determined.

Yawing moment.- The yawing-moment coefficient for any aileron deflection and wing angle of attack was essentially unaffected by variation of the Mach number. (See fig. 8.) The total yawing-moment coefficient resulting from equal up-and-down deflection of the aileron was slightly favorable (sign of yawing moment same as sign of rolling moment) at an angle of attack of approximately -4° but was adverse at angles of attack from 0° to 16°. The magnitude of the adverse yawing-moment coefficient increased as the aileron deflection and wing angle of attack increased.

Aileron hinge moments.- The variation of aileron hinge-moment coefficient with Mach number although inconsistent was generally small and, for any given wing angle of attack and aileron deflection, was generally very nearly linear. (See fig. 8.) The aileron hinge-moment parameter C_{h_α} was slightly negative and did not vary with increasing Mach number. (See fig. 9.) The parameter $C_{h_{\delta_{a_T}}}$ was also negative at all Mach numbers and became only slightly more negative as the Mach number was increased from 0.30 to 0.90.

The effects of Mach number on the hinge-moment parameters were generally similar to those reported in reference 6 for control surfaces with small trailing-edge angles on unswept wings.

Spoiler Lateral-Control Characteristics

Comparison of spoiler configurations 1 and 2.- The rolling-moment coefficients for spoiler configurations 1 and 2 at a projection of -0.07c increased with increasing Mach number or wing angle of attack. (See fig. 10.) The results further show that throughout the Mach number range investigated the spoiler at the inboard location (configuration 1) is more effective in producing rolling-moment coefficient at $\alpha = -4.2^\circ$ and 0.0° but is less effective at $\alpha = 4.0^\circ$ than the spoiler at the outboard location (configuration 2). The low-speed spoiler lateral-control results reported in reference 1 showed that throughout the complete-wing angle-of-attack range the spoiler at the more inboard location would generally give the highest rolling-moment coefficients.

The yawing-moment coefficients produced by spoiler configurations 1 and 2 were favorable (sign of yawing moment same as sign of rolling moment) throughout the Mach number range and increased in absolute magnitude as the Mach number or wing angle of attack increased. The ratio of yawing-moment coefficient to rolling-moment coefficient C_n/C_l decreased, however, as the Mach number increased. There was no consistent trend in the variation of C_n/C_l with variation of the wing angle of attack.

Rolling-moment characteristics of spoiler configuration 1.- The rolling-moment coefficient results presented in figure 11 show that spoiler configuration 1 produced favorable rolling-moments at all spoiler projections, angles of attack, and Mach numbers, although the effectiveness at small projections (-0.01c or less) was quite small at $\alpha = -4.2^\circ$. The rolling-moment coefficient increased with increasing spoiler projection, Mach number, and/or wing angle of attack. The increase in rolling-moment coefficient with spoiler projection was nearly linear at $\alpha = 0^\circ$ and 4°.

Yawing-moment characteristics of spoiler configuration 1.- The yawing-moment coefficients produced by spoiler configuration 1 were favorable throughout the projection range at all Mach numbers and wing angles of attack and generally tended to increase with increasing Mach number. The

yawing-moment coefficients also increased linearly with increasing spoiler projection. There was little effect on the spoiler yawing moment of variation of wing angle of attack. The ratio of yawing-moment coefficient to rolling-moment coefficient C_n/C_l was approximately constant throughout the projection range for any given wing angle of attack and Mach number but generally tended to decrease as either the wing angle of attack or Mach number was increased.

Comparison of lateral-control characteristics of the aileron and spoiler configuration 1.- Comparison of the aileron lateral-control data of figure 8 with the lateral-control data for spoiler configuration 1 in figure 11 shows that at any constant value of spoiler projection, the rolling-moment coefficient increased with increasing Mach number; whereas, at any constant value of total equal up-and-down aileron deflection, the rolling-moment coefficient decreased with increasing Mach number. This effect of Mach number on the rolling effectiveness of the controls was of such magnitude that with the wing at $\alpha = 0^{\circ}$ the total aileron deflection required to produce a rolling-moment coefficient equal to that produced by the spoiler at its maximum projection (-0.07c) increased from 16° at a Mach number of 0.30 to 30° at a Mach number of 0.85.

The spoiler produced favorable yawing moments as compared to the generally unfavorable yawing moments produced by the aileron. This effect, in conjunction with the normally large negative values of the stability parameter C_{l_β} (rolling moment due to sideslip) for a highly swept wing, will increase the rolling effectiveness of the spoiler and decrease the rolling effectiveness of the aileron.

CONCLUSIONS

The results of an investigation at high speeds of a semispan-wing model with an aspect ratio 3 and a leading edge swept back 51.3° to determine the wing aerodynamic characteristics and also the lateral-control characteristics of a partial-span aileron and of a stepped spoiler lead to the following conclusions:

1. The slope of the curve of lift coefficient against wing angle of attack C_{L_α} increased with increasing Mach number and the variation was in excellent agreement with the theoretical variation.

2. The wing longitudinal stability, as indicated by the slope of the curve of pitching-moment coefficient against lift coefficient $\partial C_m/\partial C_L$, increased slightly with increasing Mach number.

3. The wing drag coefficient increased slightly with increasing Mach number but the critical speed of the wing was not exceeded for any combination of lift coefficient and Mach number, even at the highest Mach number investigated (0.91).

4. The aileron rolling effectiveness decreased as the wing angle of attack and Mach number increased.

5. The total yawing-moment coefficient resulting from equal up-and-down deflection of the aileron was essentially unaffected by variation of the Mach number, and was generally adverse (sign of yawing moment opposite to sign of rolling moment).

6. The hinge-moment parameters C_{h_α} and $C_{h_{\delta_{a_T}}}$ (slope of the curves of hinge-moment coefficient with wing angle of attack and aileron deflection, respectively) were negative and varied almost negligibly with variation of the Mach number.

7. The spoiler rolling-moment coefficient increased with increasing Mach number and wing angle of attack within the small angle-of-attack range (-4° to 4°) investigated. The increase of rolling-moment coefficient with spoiler projection was nearly linear at wing angles of attack of 0° and 4°.

8. The yawing-moment coefficient resulting from spoiler projection was favorable (sign of yawing moment same as sign of rolling moment), increased with increasing spoiler projection, and tended to increase with increasing Mach number.

Langley Aeronautical Laboratory
National Advisory Committee for Aeronautics
Langley Air Force Base, Va.

REFERENCES

1. Schneiter, Leslie E., and Watson, James M.: Low-Speed Wind-Tunnel Investigation of Various Plain-Spoiler Configurations for Lateral Control on a 42° Sweptback Wing. NACA TN 1646, 1948.

2. Polhamus, Edward C.: Jet-Boundary-Induced-Upwash Velocities for Swept Reflection-Plane Models Mounted Vertically in 7- by 10-Foot, Closed, Rectangular Wind Tunnels. NACA TN 1752, 1948.

3. Herriot, John G.: Blockage Corrections for Three-Dimensional-Flow Closed-Throat Wind Tunnels, with Consideration of the Effect of Compressibility. NACA RM A7B28, 1947.

4. Polhamus, Edward C.: A Simple Method of Estimating the Subsonic Lift and Damping in Roll of Sweptback Wings. NACA TN 1862, 1949.

5. Lowry, John G., and Schneiter, Leslie E.: Estimation of Effectiveness of Flap-Type Controls on Sweptback Wings. NACA TN 1674, 1948.

6. Langley Research Staff (Compiled by Thomas A. Toll): Summary of Lateral-Control Research. NACA Rep. 868, 1947.

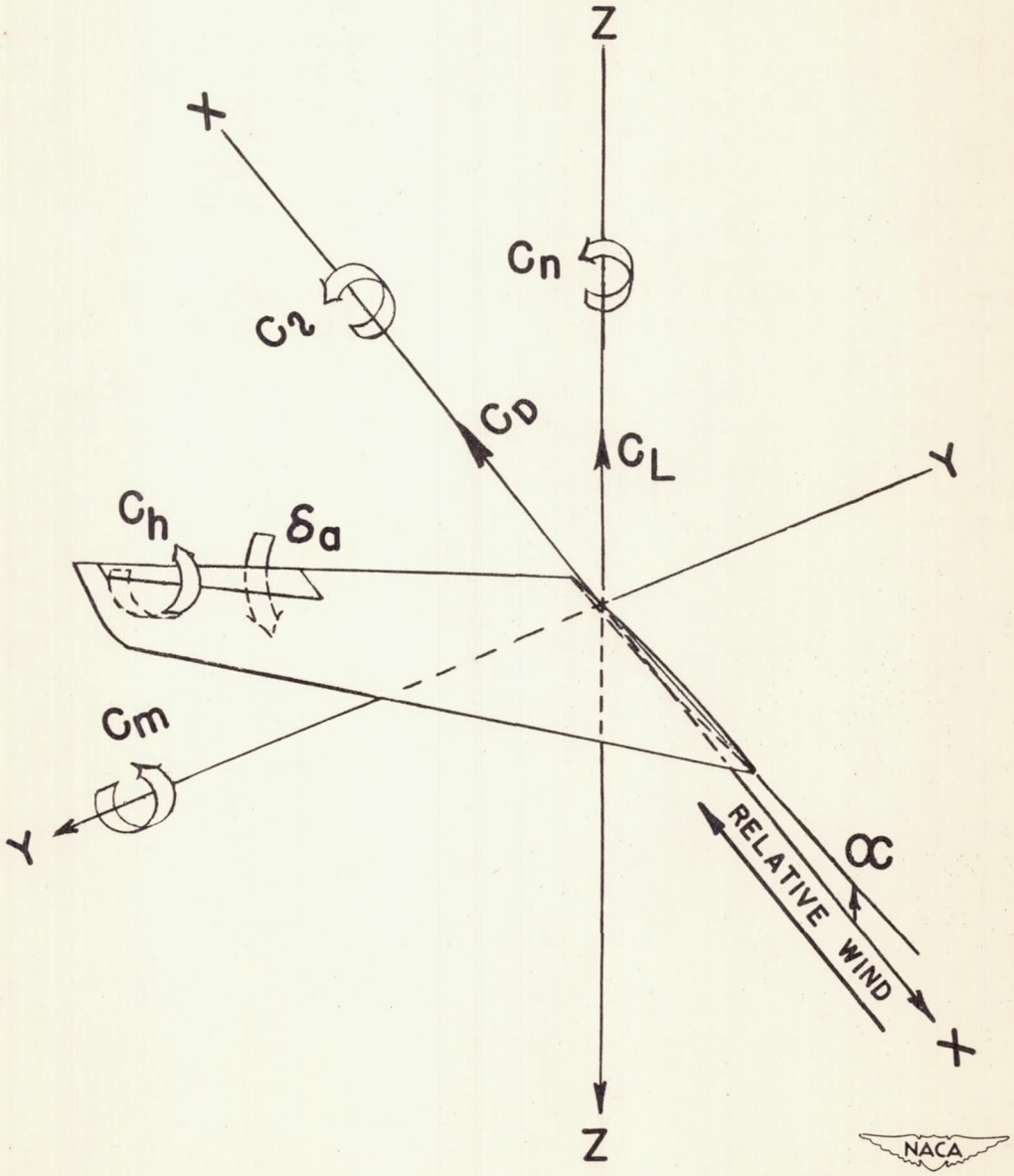

Figure 1.- System of axes, control-surface hinge moments and deflections. Positive directions of forces, moments, and deflections are as indicated by the arrows.

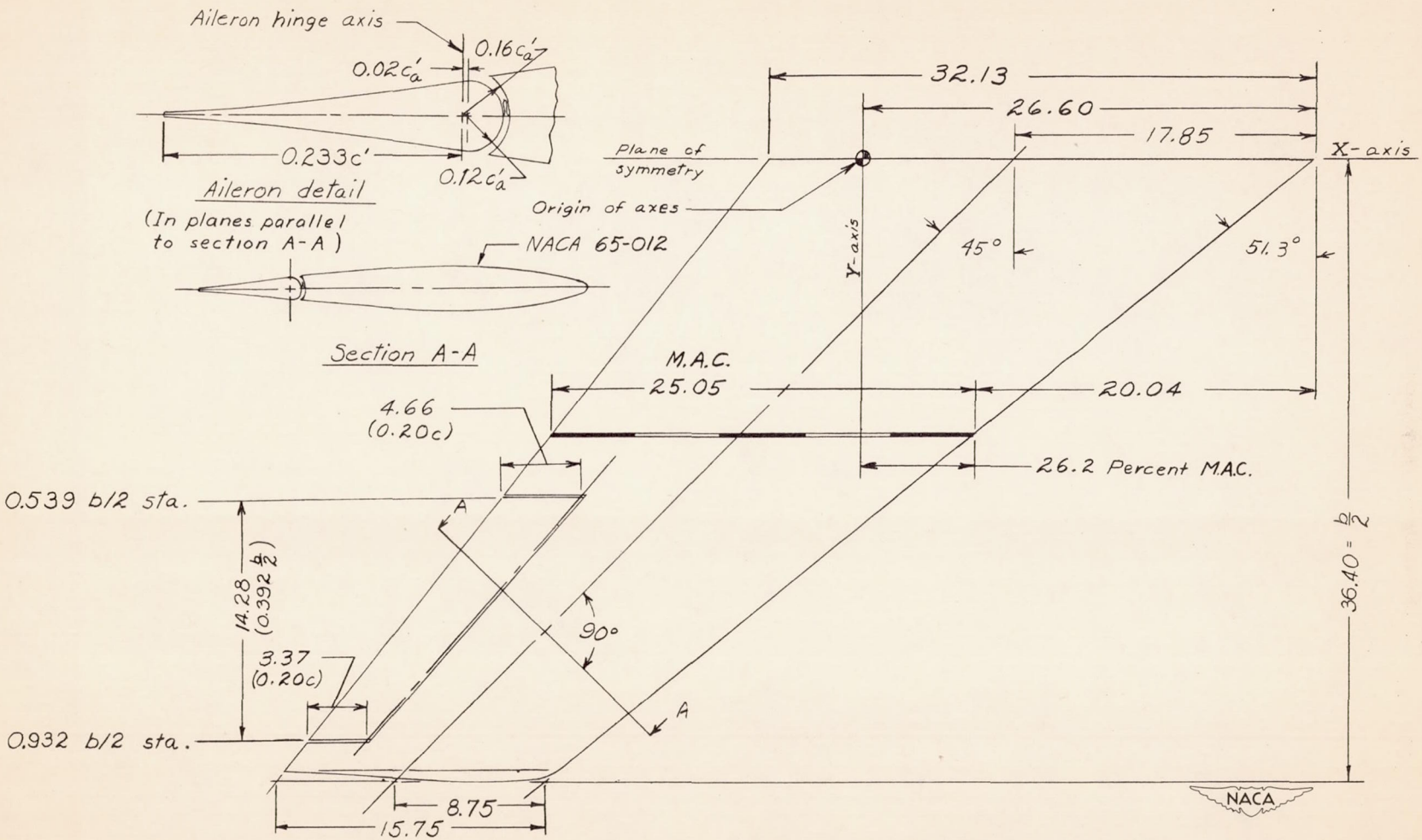

Figure 2.– Drawing of the 51.3° sweptback wing model. A = 3.06; S = 12.06 square feet; taper ratio = 0.49. (All dimensions are in inches unless otherwise noted.)

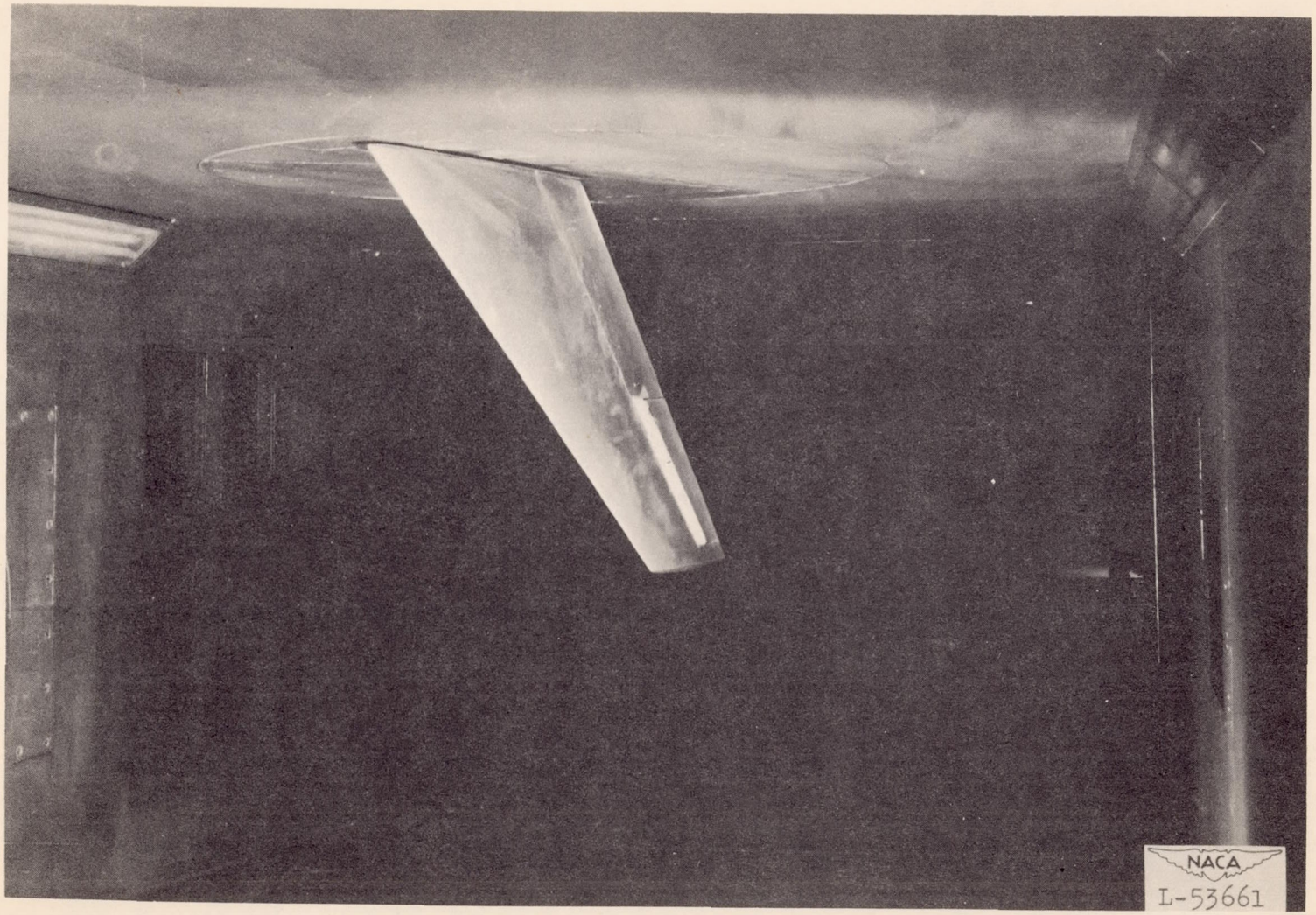

Figure 3.- The 51.3° sweptback semispan wing model mounted from the ceiling of the Langley high-speed 7- by 10-foot tunnel.

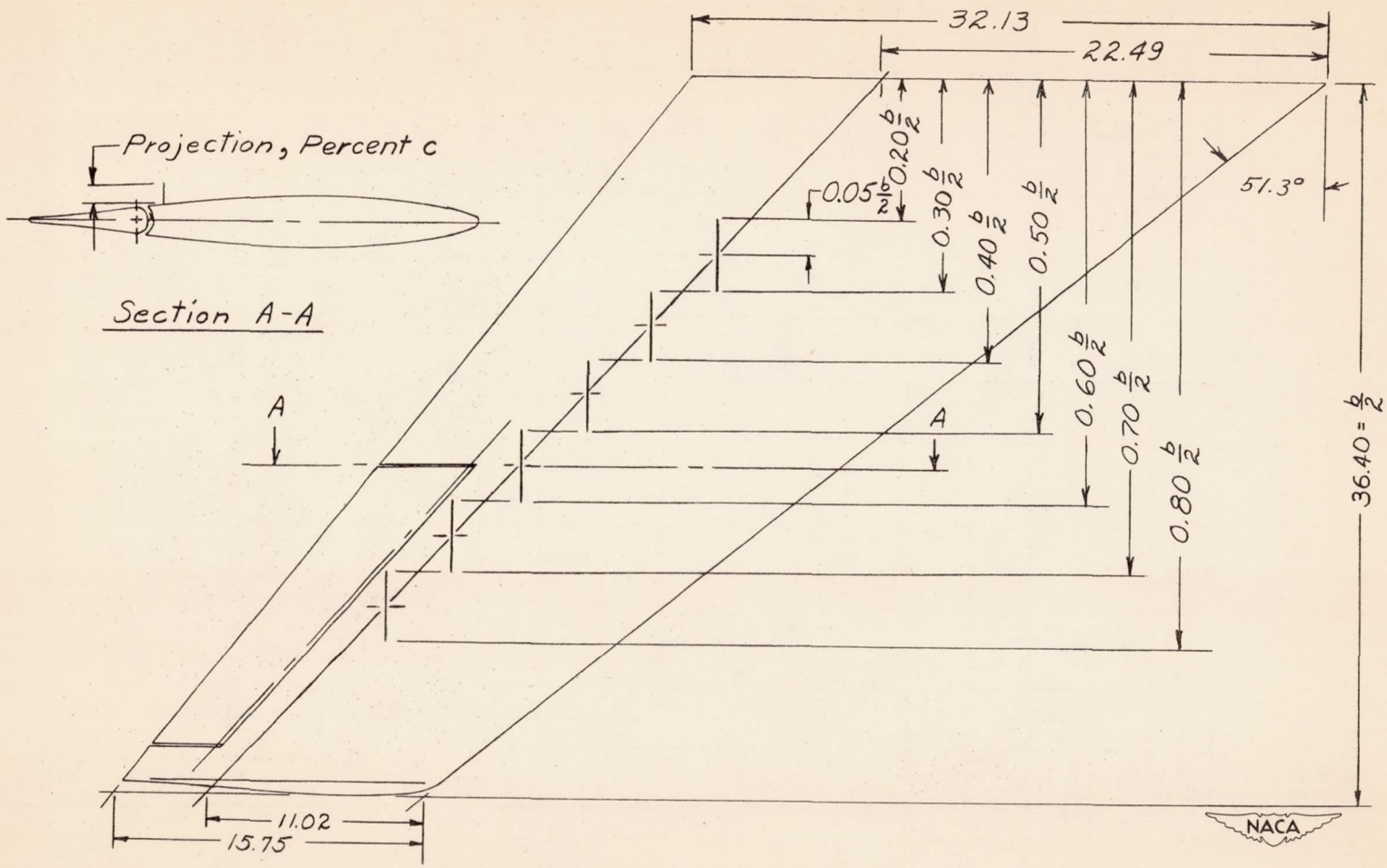

Figure 4.– Sketch of spoiler configuration 1 on 51.3° sweptback wing. Spoiler segments for spoiler configuration 2 were located in a similar manner along 0.70c line from the $0.30\frac{b}{2}$ to the $0.90\frac{b}{2}$ wing stations. (All dimensions are in inches unless otherwise noted.)

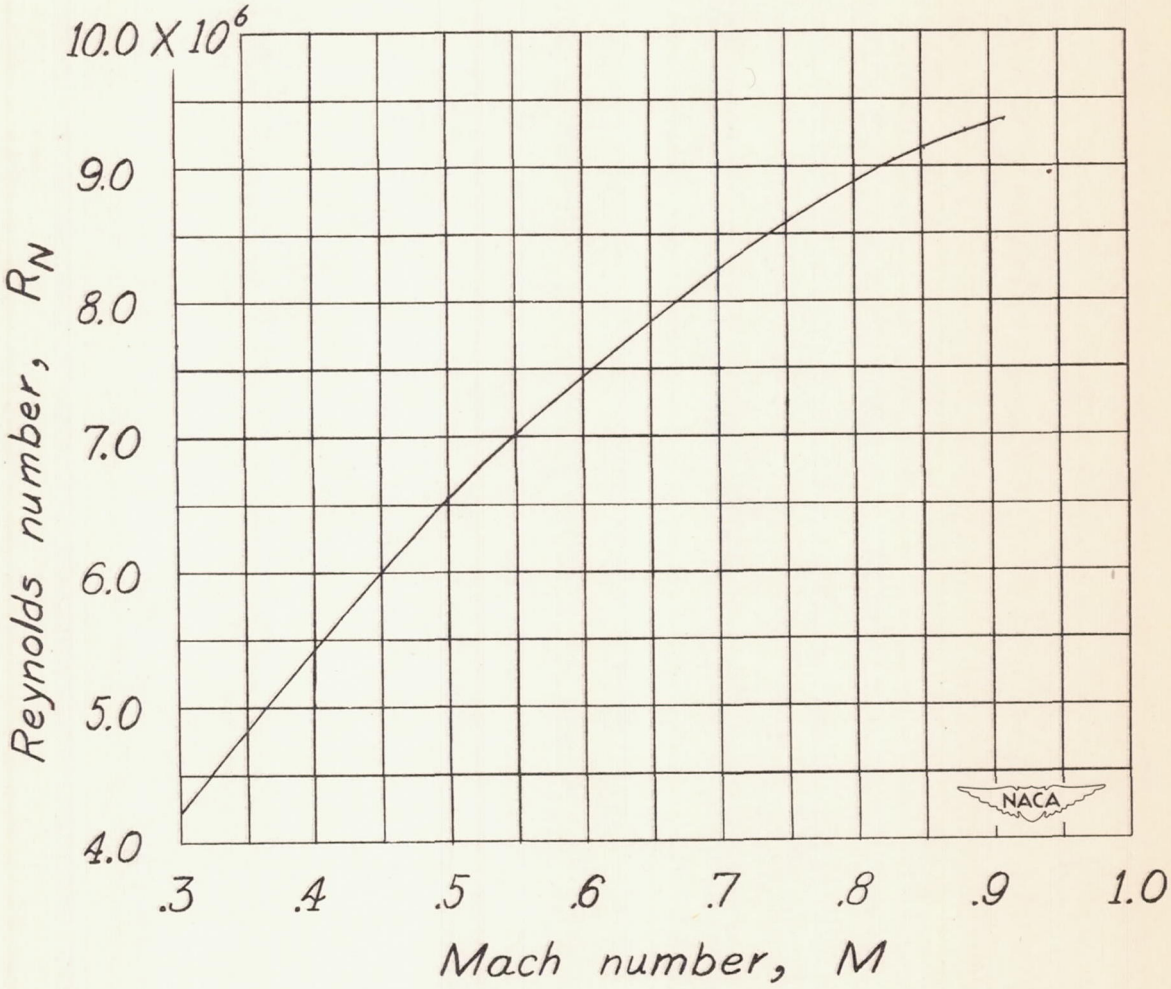

Figure 5.- Variation of Reynolds number with Mach number. Reynolds number is based on wing mean aerodynamic chord of 2.087 feet.

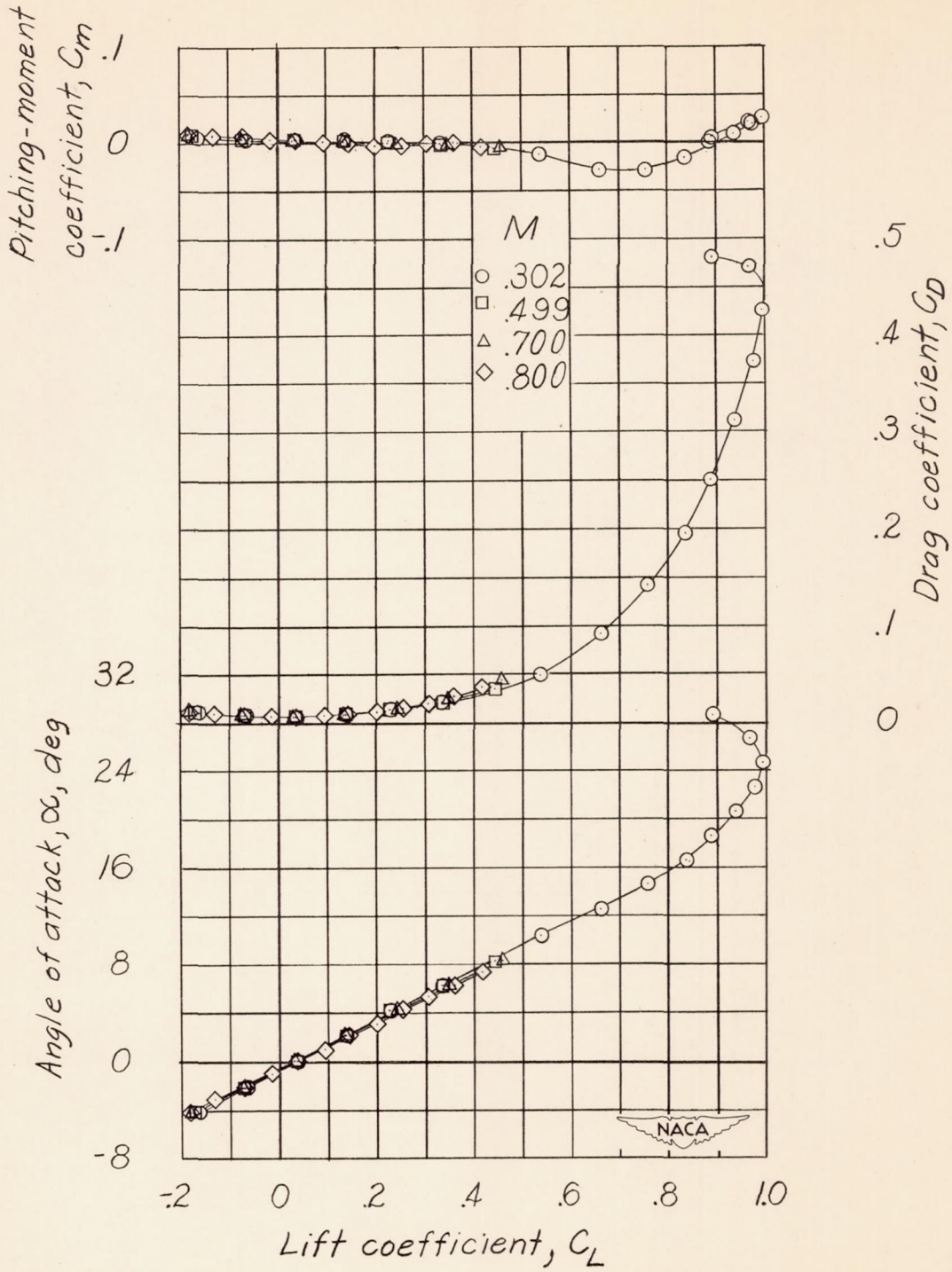

(a) Mach numbers from M = 0.302 to M = 0.800.

Figure 6.– Wing aerodynamic characteristics and aileron hinge-moment characteristics with $\delta_{a_{ave}} = 0^{\circ}$ for various Mach numbers.

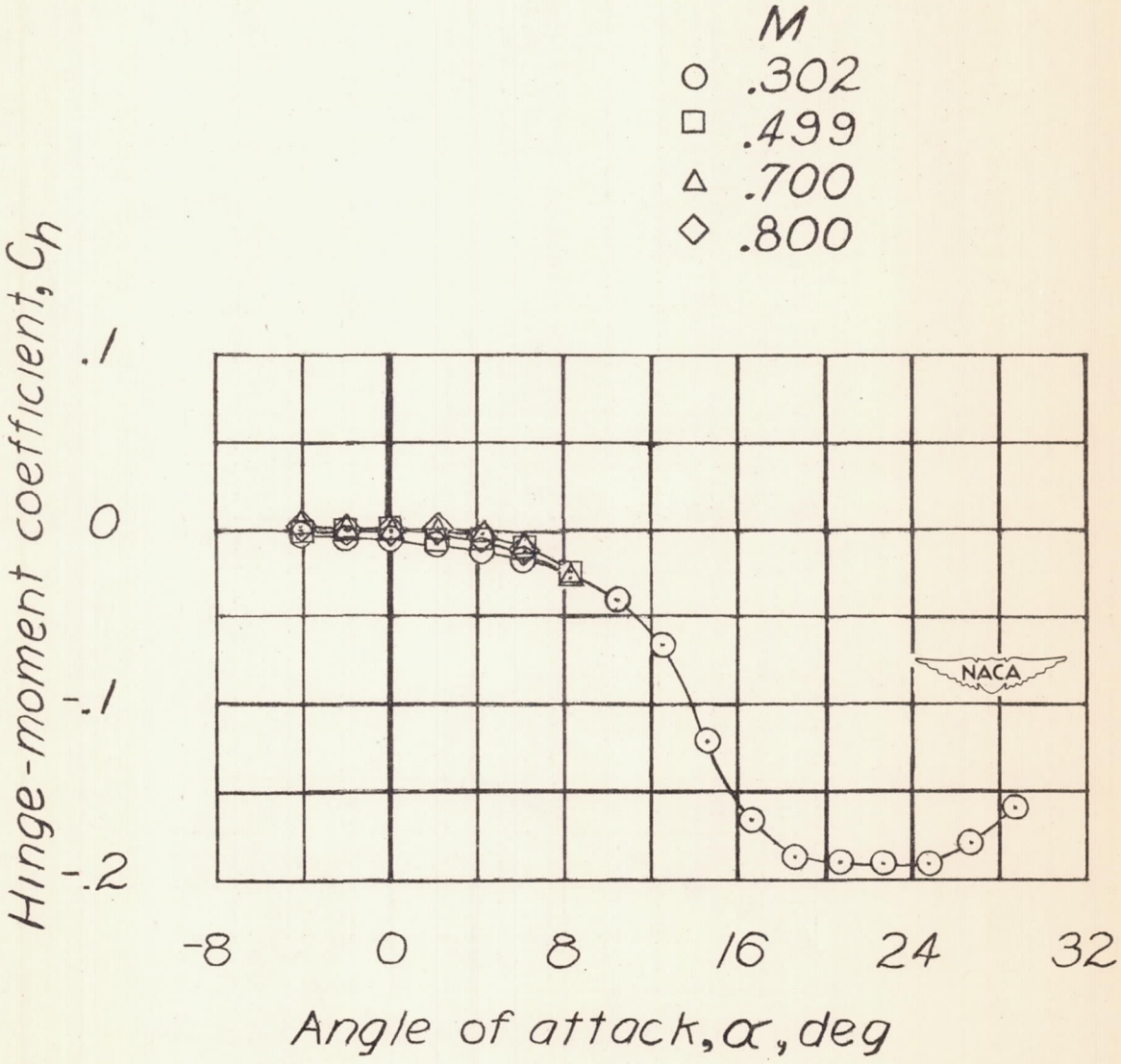

(a) Concluded.

Figure 6.– Continued.

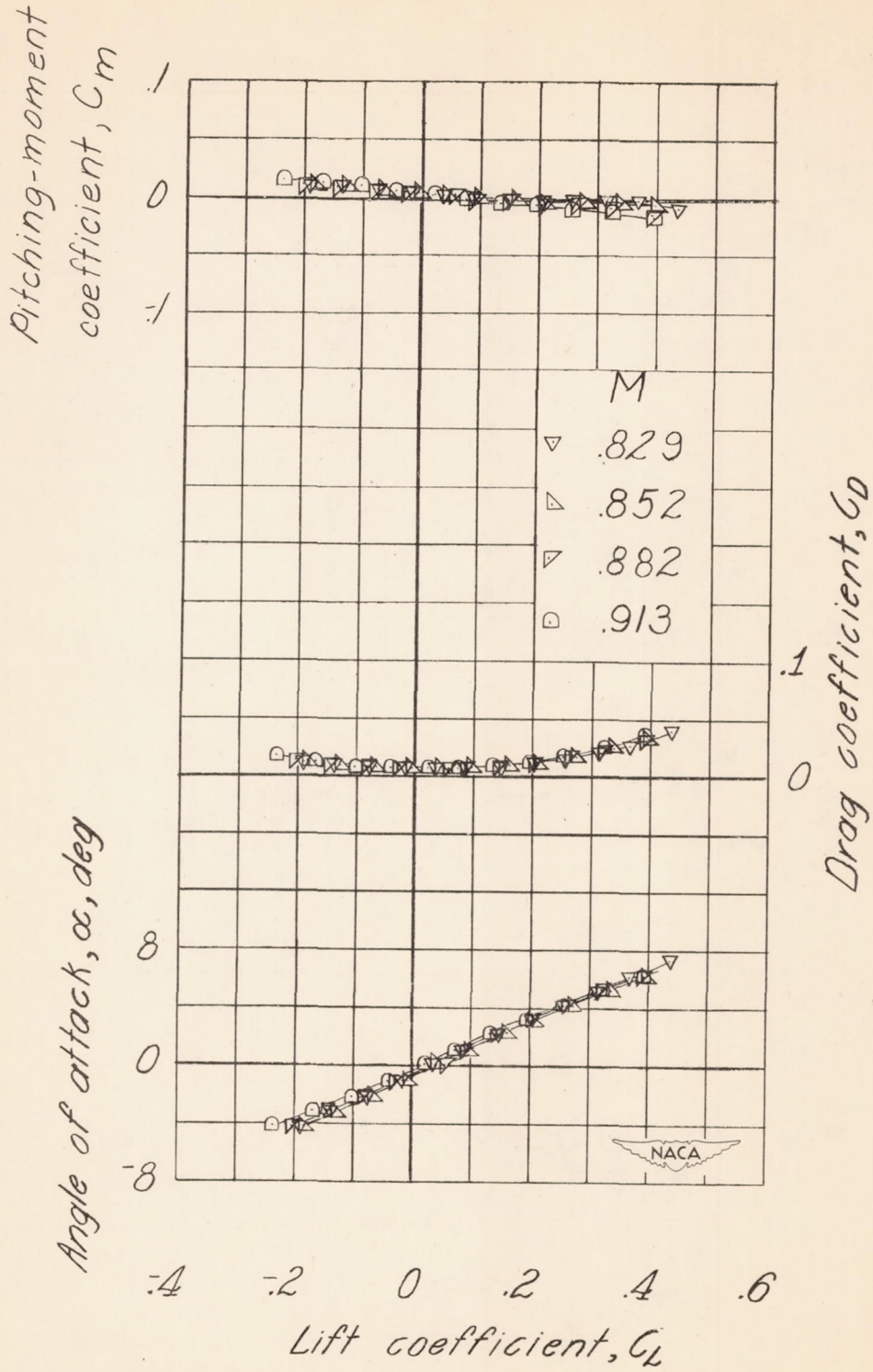

(b) Mach numbers from M = 0.829 to M = 0.913.

Figure 6.– Continued.

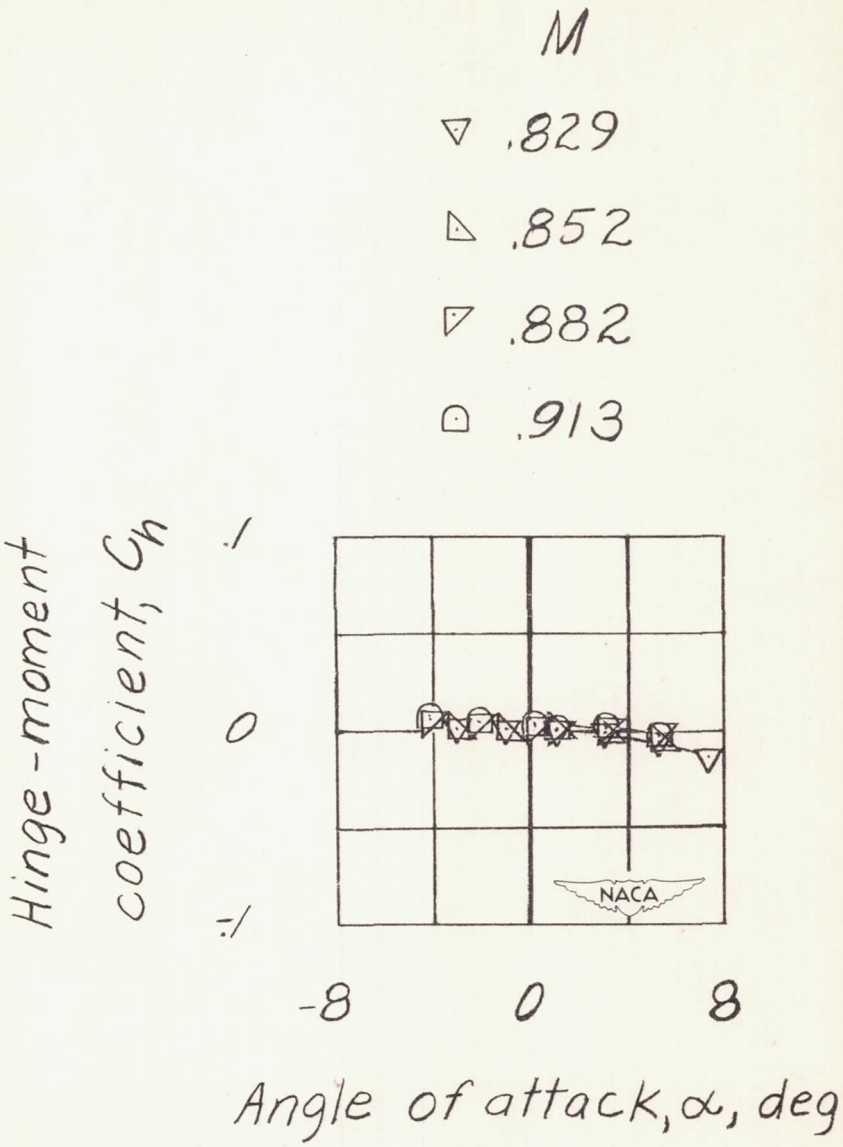

(b) Concluded.

Figure 6.– Concluded.

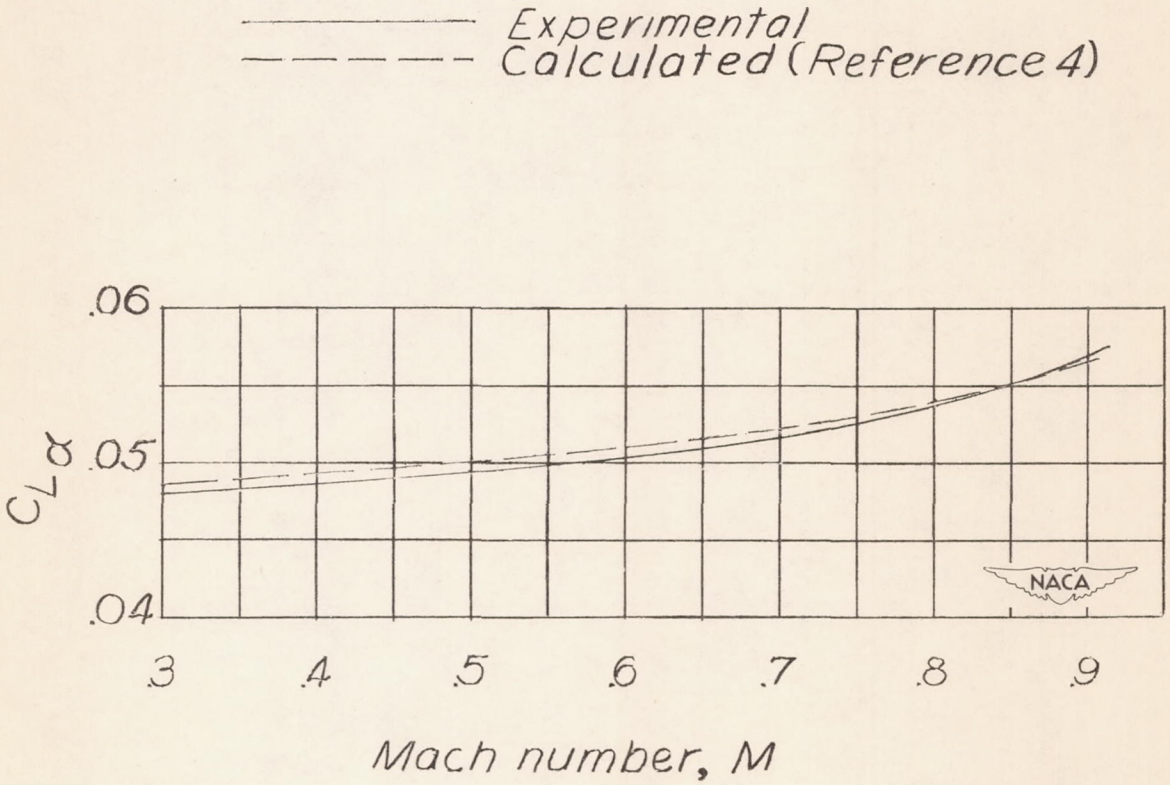

Figure 7.- Experimental and theoretical variation of the wing lift-curve slope C_{L_α} with Mach number.

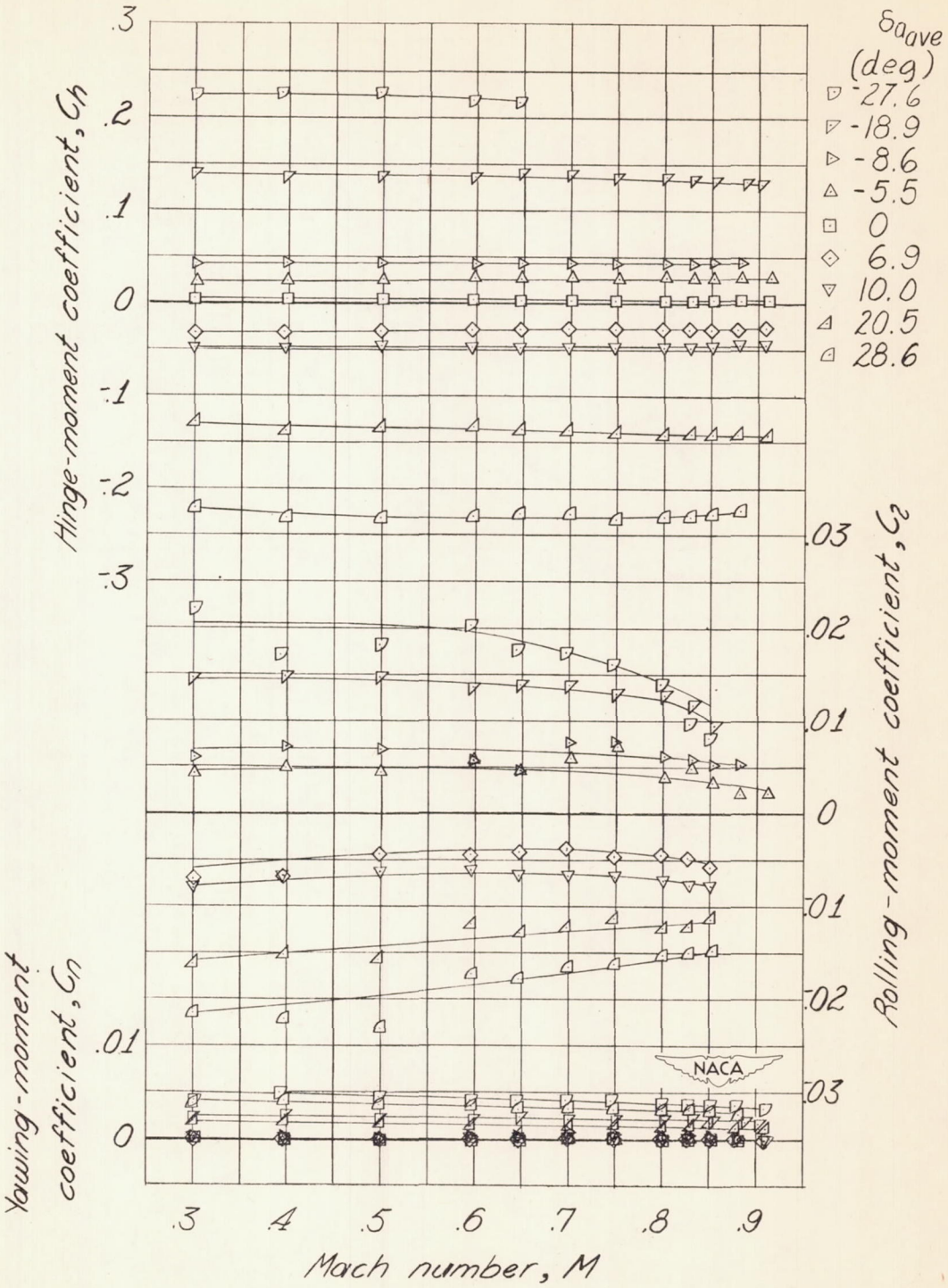

(a) $\alpha = -4.0^{\circ}$.

Figure 8.– Variation of aileron lateral-control characteristics with Mach number for various aileron deflections.

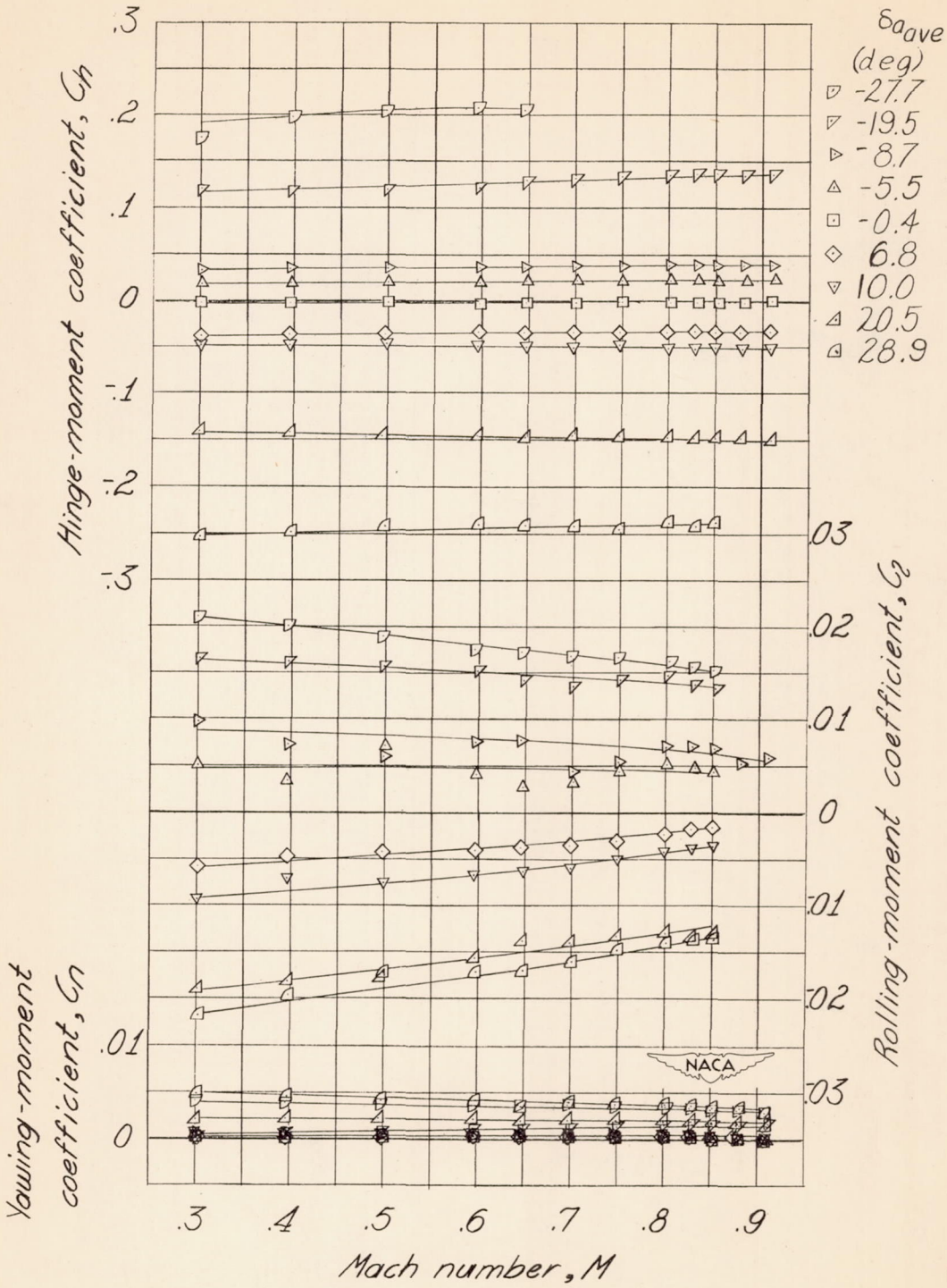

(b) $\alpha = 0.0^{\circ}$.

Figure 8.– Continued.

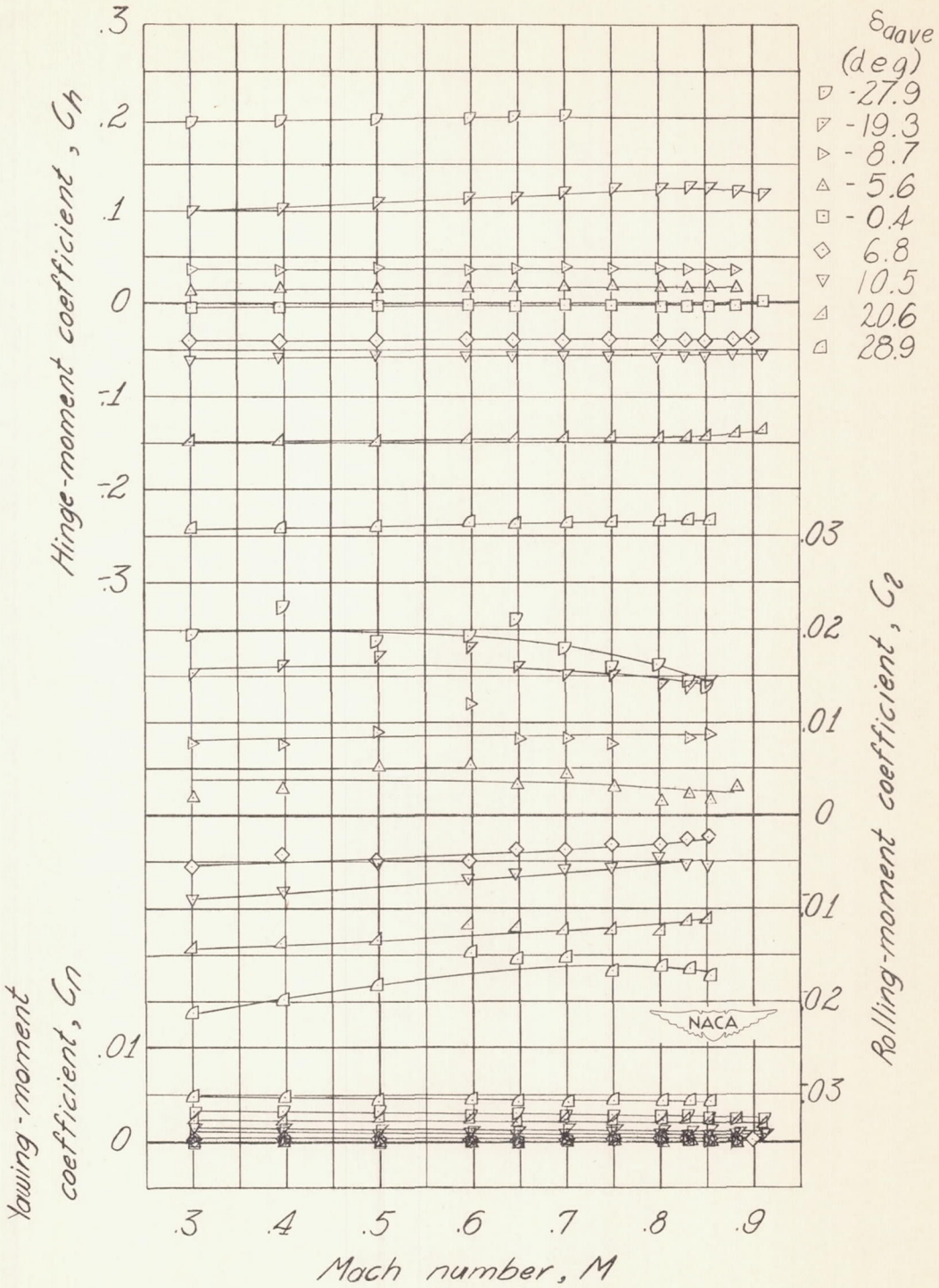

(c) $\alpha = 4.2^{\circ}$.

Figure 8.– Continued.

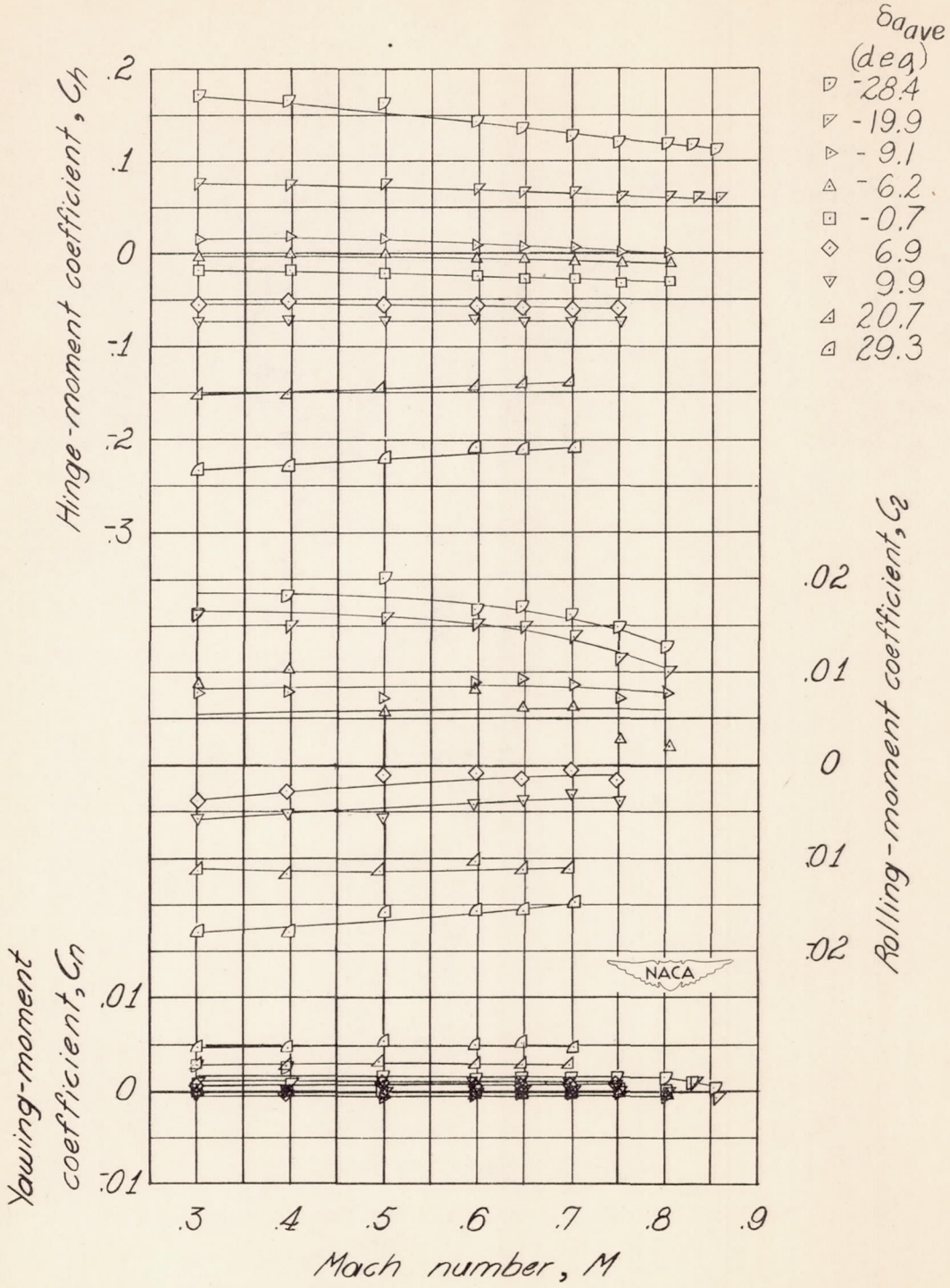

(d) $\alpha = 8.2^{\circ}$.

Figure 8.– Continued.

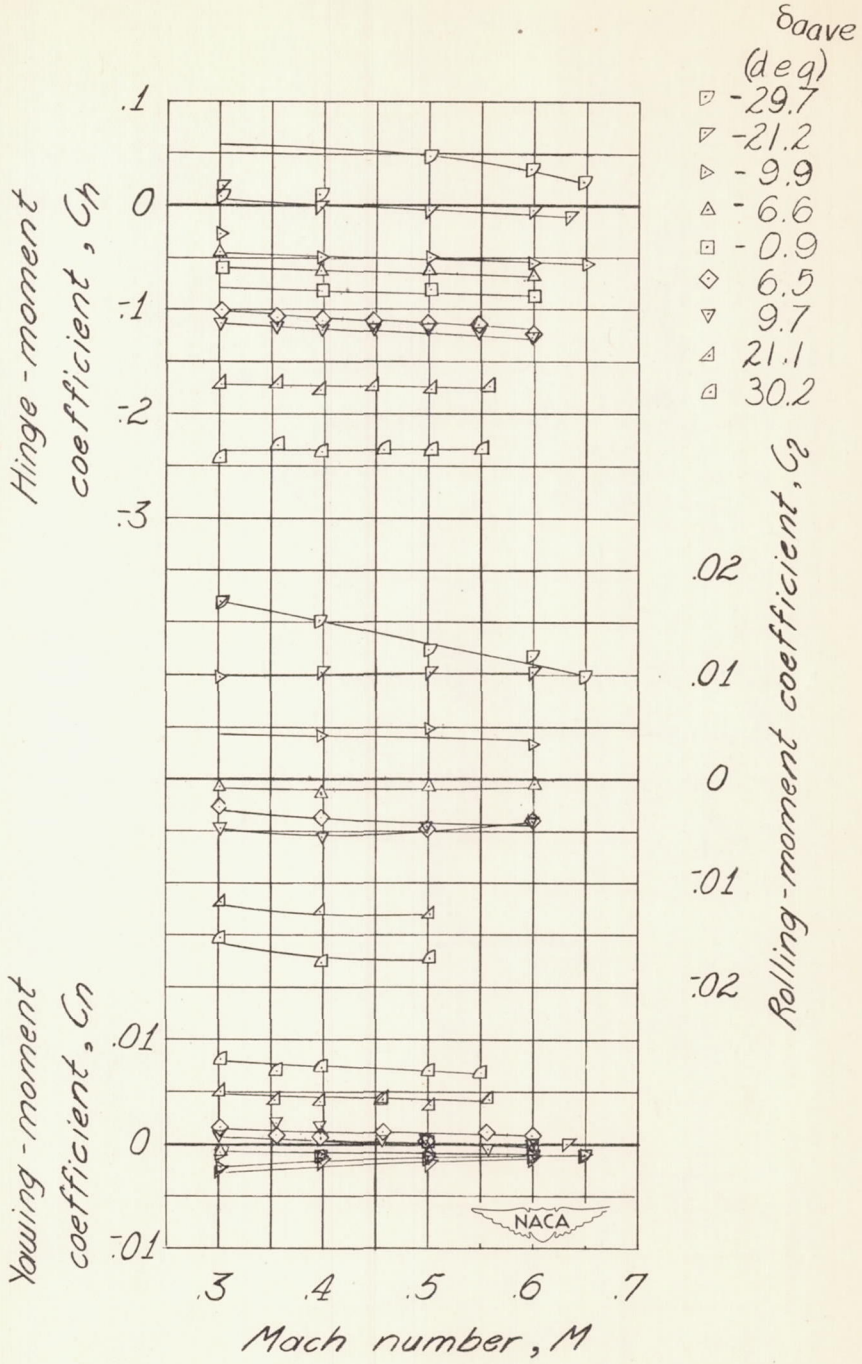

(e) $\alpha = 12.3^{\circ}$.

Figure 8.– Continued.

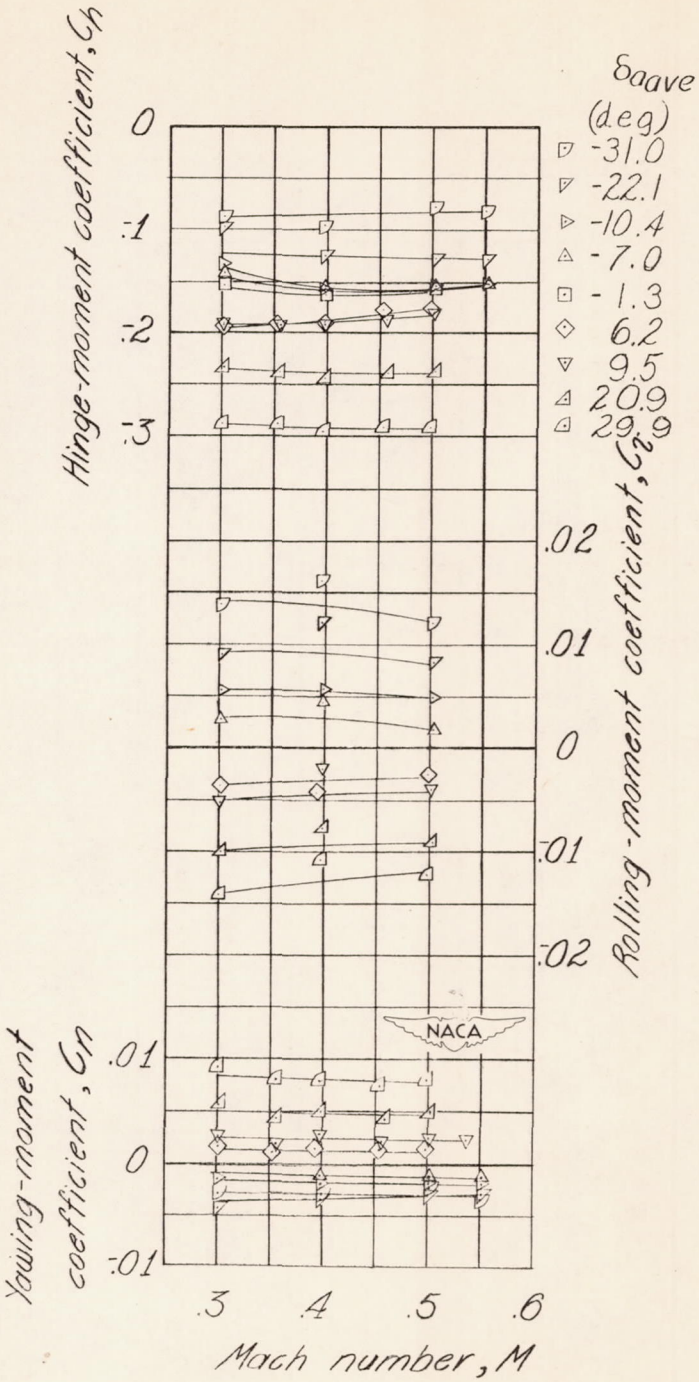

(f) $\alpha = 16.4^{\circ}$.

Figure 8.– Concluded.

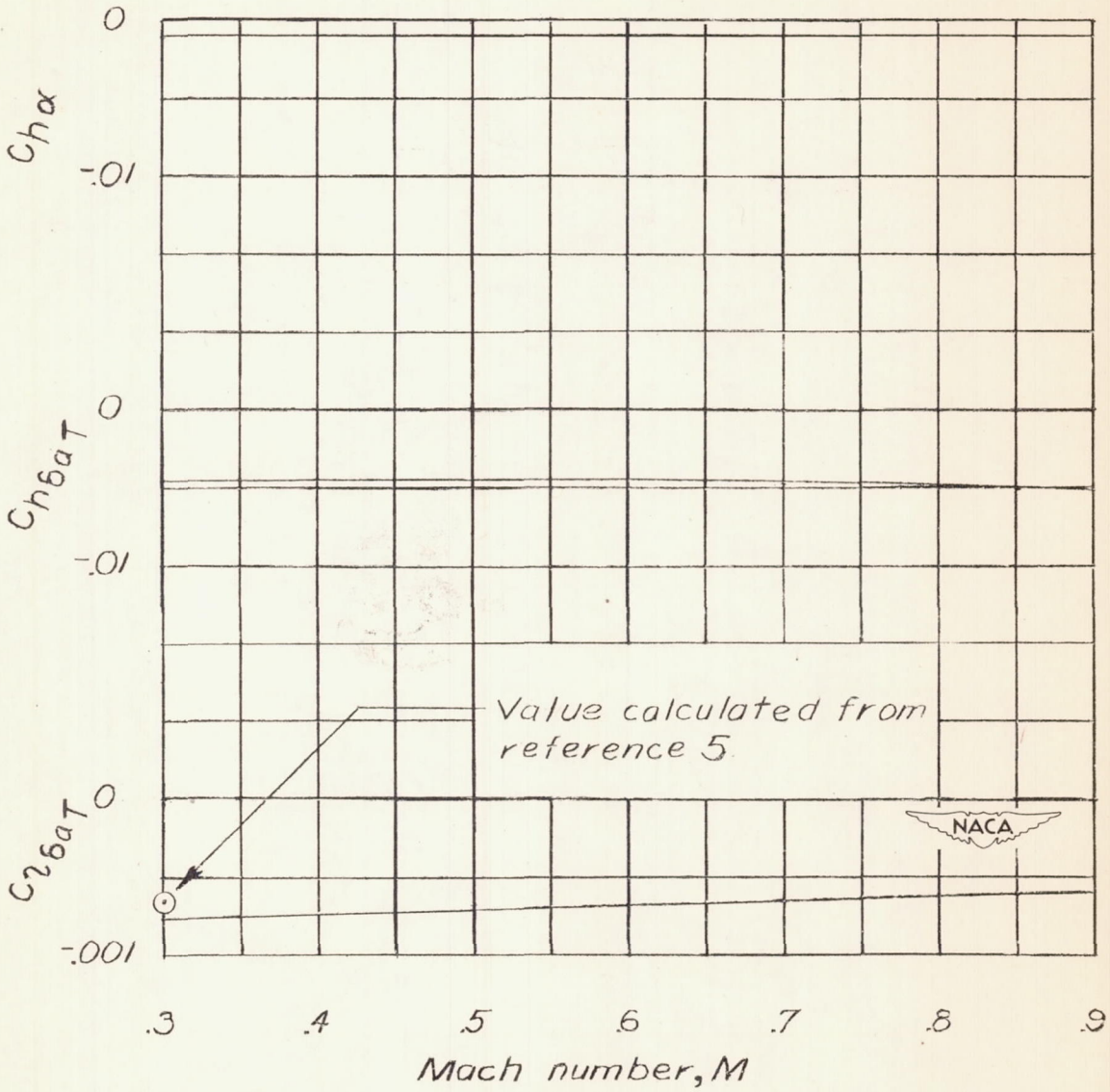

Figure 9.- Variation of the aileron lateral-control parameters C_{h_α}, $C_{h_{\delta_{a_T}}}$, and $C_{l_{\delta_{a_T}}}$ with Mach number.

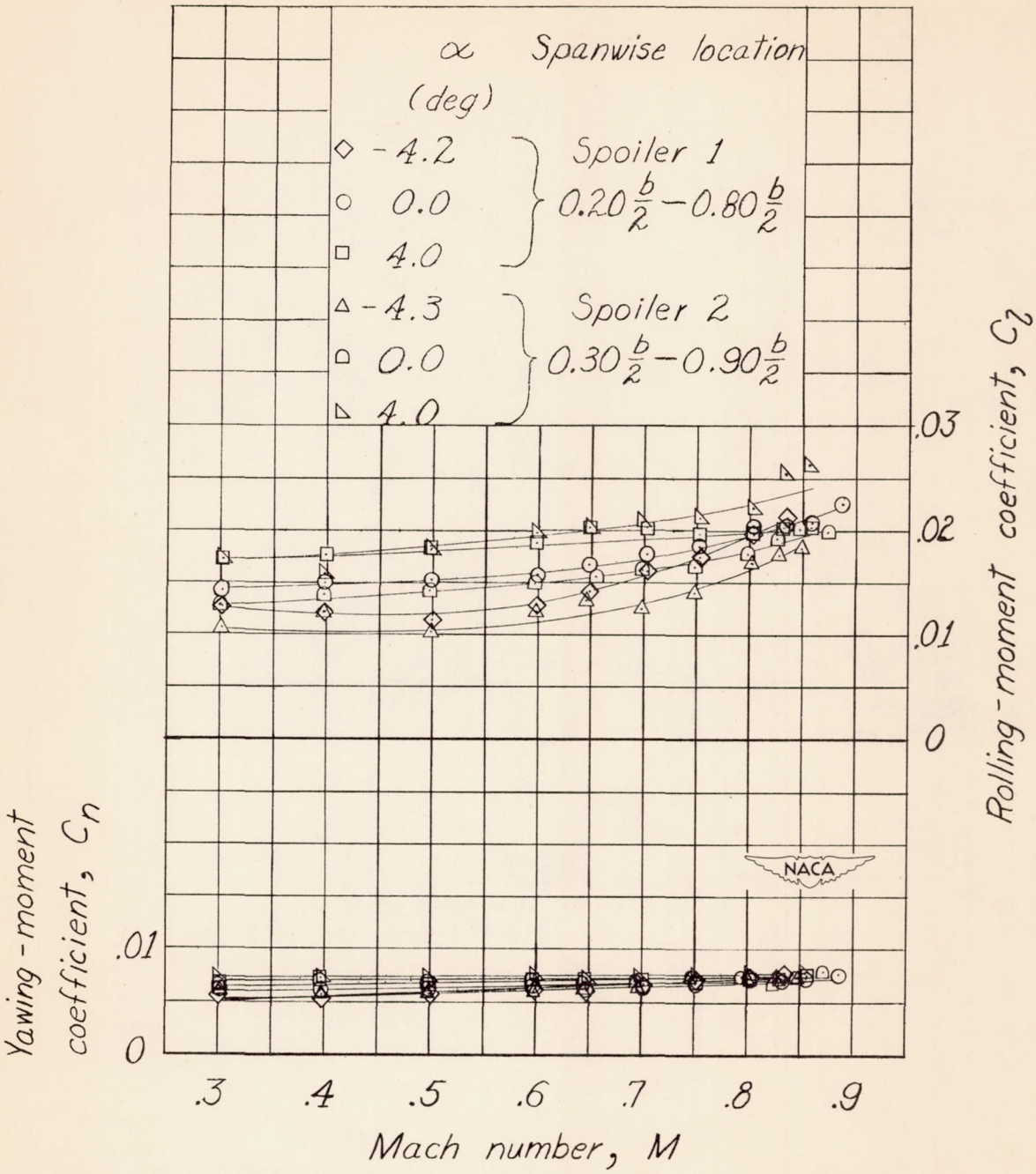

Figure 10.– Effect of spanwise location of the spoiler on the variation of spoiler rolling-moment and yawing-moment coefficients with Mach number and angle of attack. Spoiler projection = –0.07c.

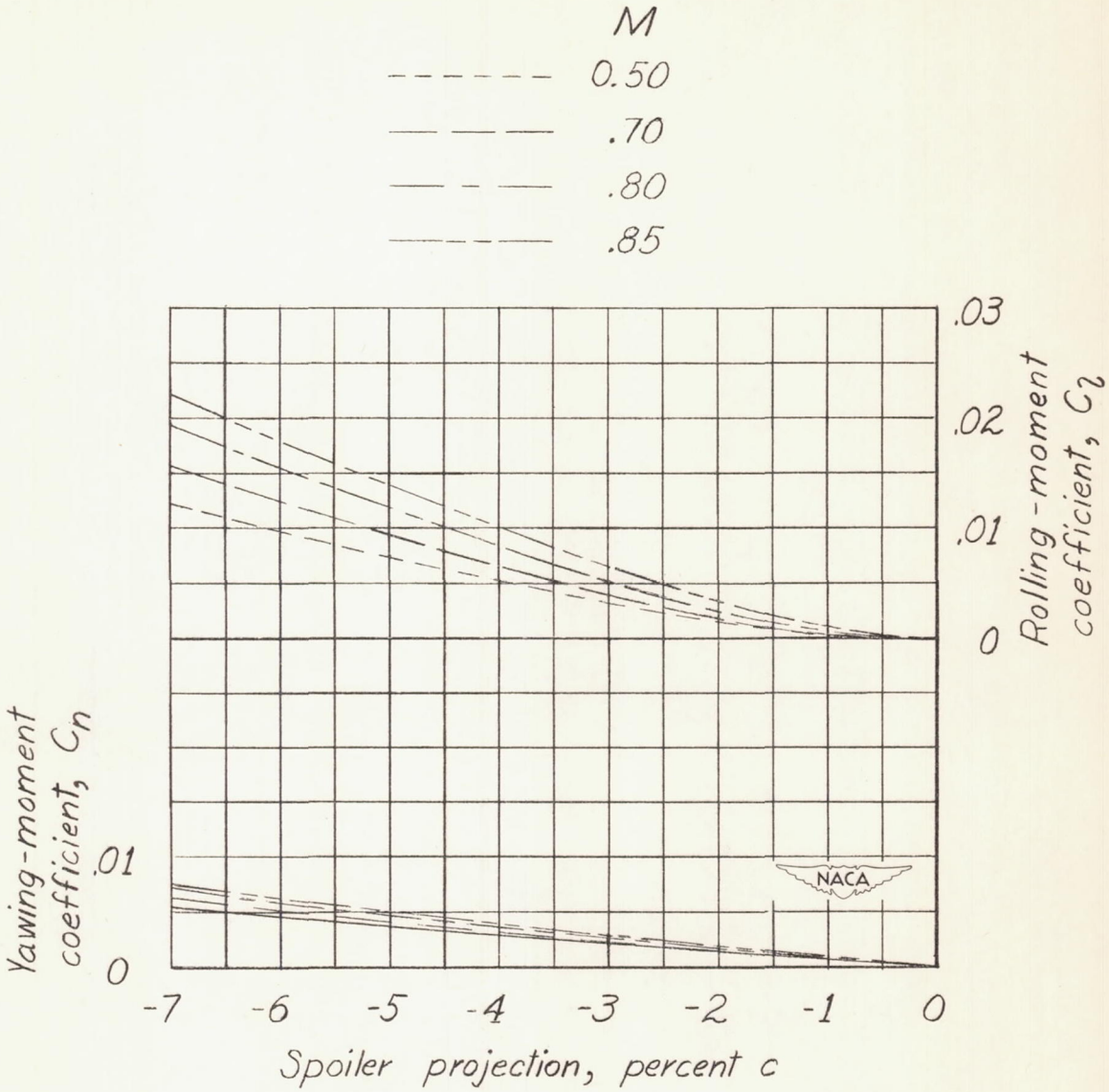

(a) $\alpha = -4.2^{\circ}$.

Figure 11.- Variation of rolling-moment and yawing-moment coefficient with spoiler projection for various Mach numbers. Spoiler configuration 1.

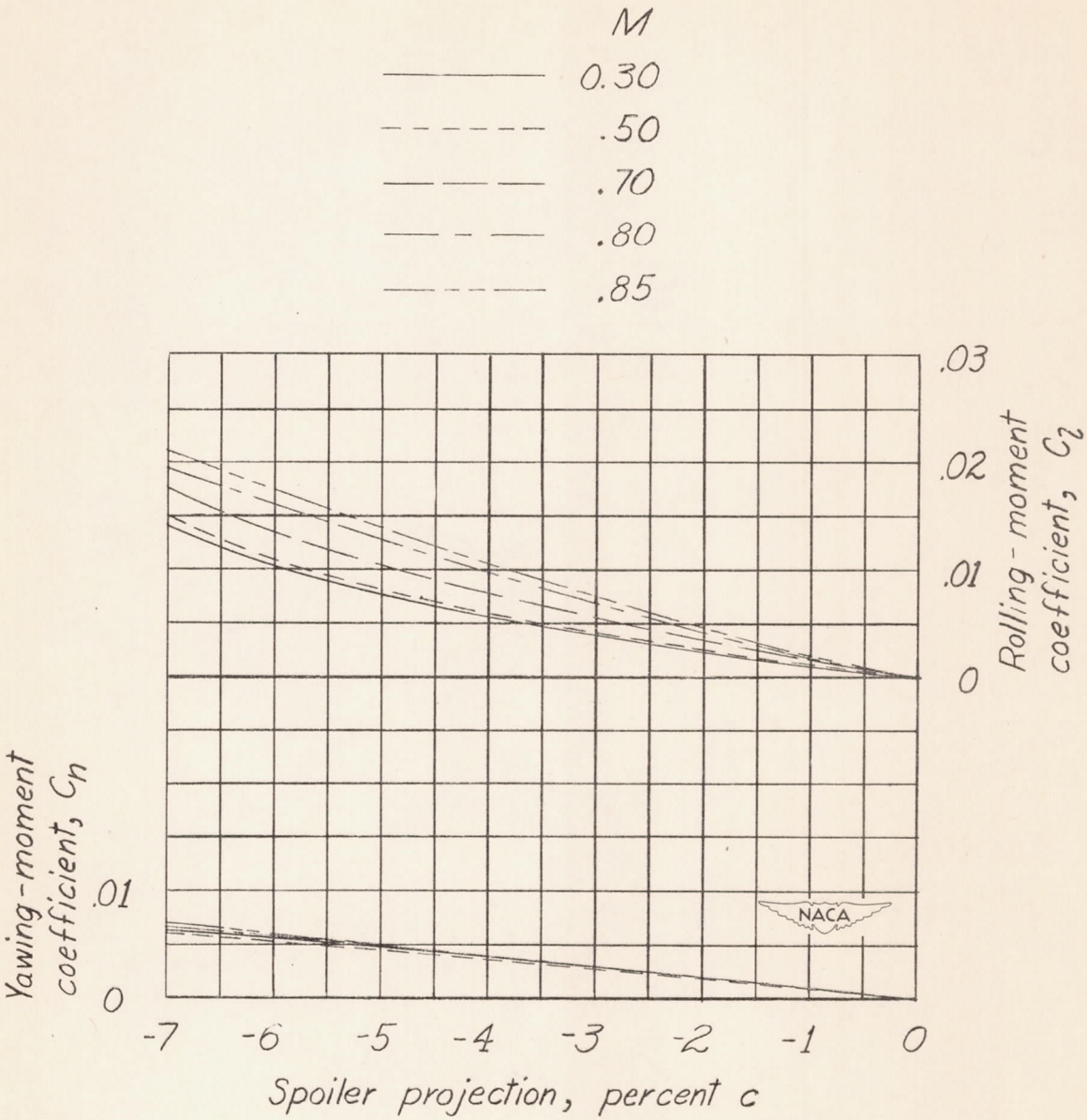

(b) $\alpha = 0.0^{\circ}$.

Figure 11.– Continued.

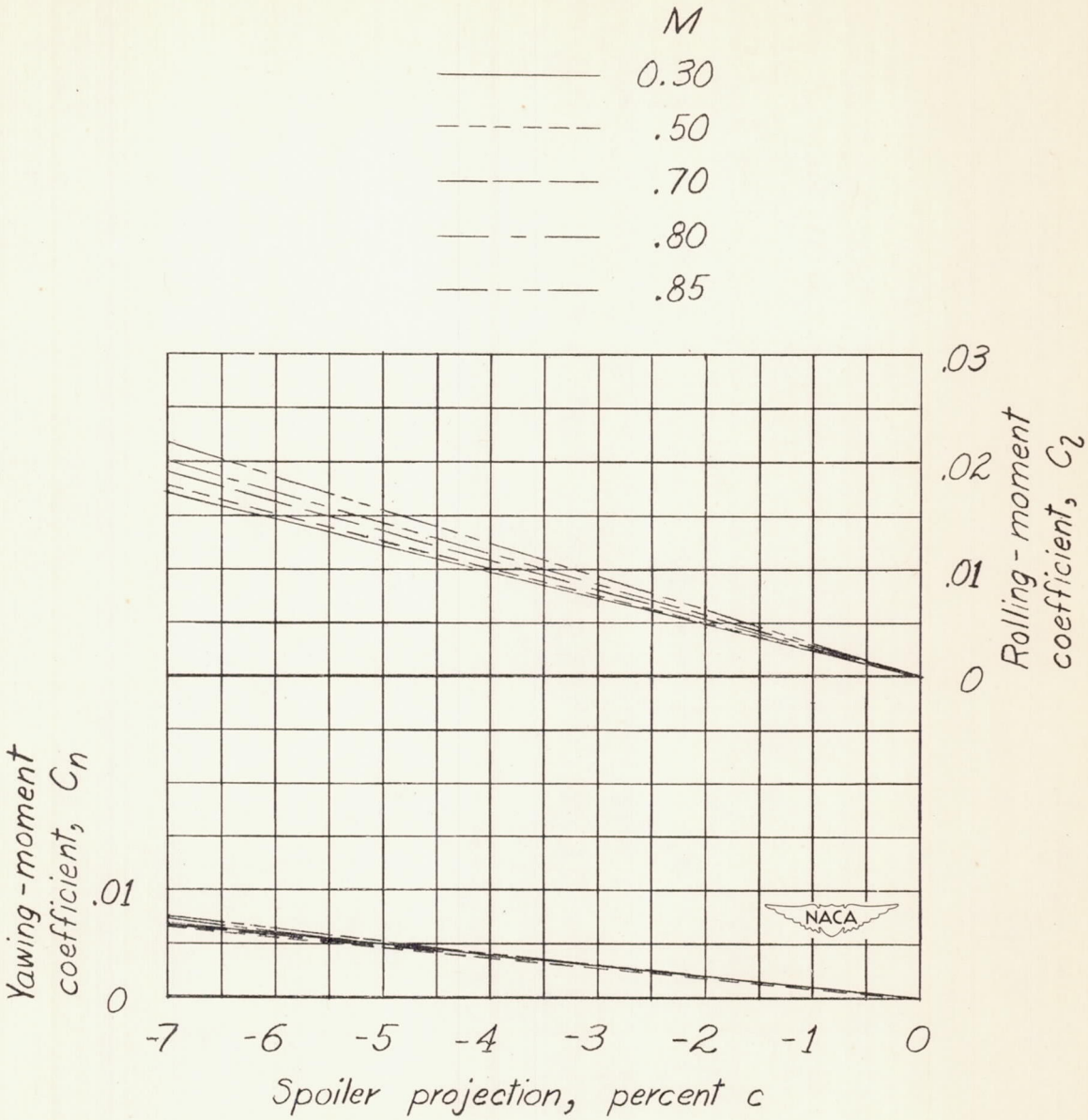

(c) $\alpha = 4.0^{\circ}$.

Figure 11.– Concluded.